eTETRAS: An Extension To The Essential Tremor Rating Assessment Scale

by

Jonathan Ting

A thesis submitted to the Graduate Faculty of
Auburn University
in partial fulfillment of the
requirements for the Degree of
Master of Science

Auburn, Alabama
August 3, 2024

Keywords: Tremor, Machine Learning, Sensors

Approved by

Brendon Connor Allen, Chair, Assistant Professor of Mechanical Engineering
Chad Gregory Rose, Assistant Professor of Mechanical Engineering
Scott Martin, Assistant Professor of Mechanical Engineering

Abstract

Essential tremor (ET) is a widespread neurological condition characterized by tremors in an individual's limbs, significantly impacting one's quality of life. It stands as the most prevalent type of movement disorder, often leading to debilitating effects. Various scales, such as the Fahn-Tolosa-Marin (FTM) tremor rating scale and The Essential Tremor Rating Assessment Scale (TETRAS), have been developed and used by physicians to classify the severity of ET. While the FTM scale is highly utilized in ET severity diagnosis, it relies on subjective assessments of the tremor. TETRAS, on the other hand, provides a more quantitative analysis of ET severity by ranking the severity of the tremor based on tremor magnitude and addresses the shortcomings of FTM. Though TETRAS is seen as an improvement to FTM, both scales often lack the necessary resolution and granularity for optimal diagnosis and treatment. Moreover, ET severity rating scales like TETRAS require a trained professional (such as a neurologist) to be present, and even in such cases, physicians use TETRAS as a metric baseline to visually approximate the severity of the tremor. This reliance on manual approximations by clinical personnel may introduce inconsistencies and bias due to variability in technique and accuracy, diminishing proper assessment and subsequent treatment. To address the limitations of TETRAS, an extended version of TETRAS (eTETRAS) was developed that leverages machine learning and wearable sensors to quantify ET severity across the entire joint range of motion. Specifically, the proposed eTETRAS utilizes a deep neural network (DNN) to classify ET severity over the range of motion of the affected limb using joint angle measurements, eliminating the need for a clinician diagnosis. To enable a rapid DNN response (i.e., nearly real-time ET classification) with enhanced resolution, the DNN assesses the severity of ET every 0.5 second increment. After the second iteration of eTETRAS, the DNN-based classifier achieved a training accuracy of 99.59% and 100%

for the simulated and experimentally obtained datasets, respectively. Moreover, eTETRAS attained a training accuracy of 99.65% when trained using the combined simulation and experimental dataset.

In Chapter 1, an overview of TETRAS and its key issues are presented. This discussion serves as a foundation for exploring the motivation, clinical efficacy, and intellectual merit of the proposed eTETRAS classifier, which incorporates a comprehensive literature review. Chapter 2 discusses the ET signal generation and the experimental protocol. Chapter 3 proposes and tests a preliminary version of eTETRAS. This includes a single-dimensional DNN that uses knee encoder data as inputs into the DNN. Chapter 4 advances the work in Chapter 3 by presenting and testing the latest iteration of eTETRAS, which includes joint stiffness data concurrently with knee encoder measurements as inputs into the DNN to create a two-dimensional DNN. In Chapter 5, the thesis is concluded by highlighting the clinical and intellectual contributions of eTETRAS, and its future developments.

Acknowledgments

I would like to give my deepest thanks to Dr. Brendon Allen for his unwavering support and mentorship. His guidance has been vital in shaping my research and professional growth. I would also like to thank Dr. Chad Rose for his support and guidance throughout my academic career. I am truly fortunate to work with such patient and insightful people. Also, I would like to thank current and past member of the WeBR and CARE labs for their guidance, patience, and dedication. I would also like to thank my family and my friends for their unwavering support throughout my graduate career for they have shaped me as the person I am today. I am profoundly grateful for their patience, encouragement, and belief in my abilities.

Table of Contents

List of Figures

List of Tables

List of Abbreviations

AI	Artificial Intelligence
DNN	Deep Neural Network
ET	Essential Tremor
eTETRAS	extension to The Essential Tremor Rating Assessment Scale
FTM	Fahn-Tolosa-Marin
PoI	Points of Interest
ReLU	Rectified Linear Unit

Chapter 1

Introduction

Essential tremor (ET) is one of the most common types of movement disorders that cause tremor [1, 2, 3]. As it stands, ET affects an estimated 350 million adults over 40 years of age worldwide [2]. This condition is characterized by rhythmic and involuntary shaking of an individual's limbs during task specific activities, increasing the risk of injury and diminishing independence and quality of life [1]. In fact, as a result of an aging population, there is expected to be a significant increase in the occurrence of ET and Parkinson's disease within the general population [4]. This growing concern over the increasing incidence of ET and Parkinson's disease highlights the urgency for the enhancement of ET treatment and prevention. Yet, despite years of active research, the onset and evolution of ET is not yet thoroughly understood; therefore, comprehensive treatments and therapies to alleviate the debilitating effects of ET are still being actively developed and investigated [3]. The most promising treatment plans currently studied involve patient-specific combinations of physical and pharmacological interventions, the development of which necessitate continual assessment of ET severity and progression by clinicians [3]. However, the diagnosis of ET severity often relies on subjective methods, making ET severity diagnosis susceptible to bias caused by various factors such as the availability of specific tools, differences in procedural approaches, and variations in the instruction provided for a given method's use [5]. These diagnostic methods include simple clinical observation, standardized rating scales, or the subjective assessment of drawn figures, all of which can introduce variability in ET severity diagnosis [5].

1.1 The Essential Tremor Rating Assessment Scale (TETRAS)

One of the issues with diagnosing ET is the lack of stringent diagnostic criteria, which introduces errors and bias, consequently impeding the diagnosis of ET [6]. One of the earliest and most commonly utilized scales for classifying the severity of ET is the Fahn-Tolosa-Marin tremor rating scale, which establishes a metric baseline for physicians to visually approximate the severity of ET [7]. Yet, despite the wide use of FTM in tremor severity analysis, FTM spans a narrower range of tremor amplitudes, potentially resulting in a ceiling effect in studies involving more severe ET [8]. Developed as a standardized metric for diagnosing ET severity similar to FTM, TETRAS is a recently established ET classification scale, which aims to reduce diagnostic variability by establishing a metric baseline for diagnosing tremor severity. However, unlike FTM, TETRAS enables physicians to visually approximate the severity of ET across a broader spectrum of tremor amplitudes [9, 10, 11]. In clinical practice, TETRAS involves manual, centimeter-precision measurements of limb deviation from their neutral positions during tremors [11]. As stated in [11], TETRAS can be used to evaluate head, face, upper limb and lower limb tremors, by scoring the tremor movement from 0-4, with 0 indicating no tremor and 4 indicating the most severe tremor. This thesis primarily focuses on lower limb ET, which impedes balance and mobility during daily activities; thus, increasing the risk of injuries caused by and resulting from falling. Table 1.1 presents the metric measurements to rate lower limb ET using TETRAS, which is assessed bilaterally through heel-shin movement. In this thesis, the severity score for ET is determined by highest and lowest peak deviations observed across the complete sequence of tremor movements occurring within a specific time-frame, similar to [11].

A unique feature of TETRAS compared to other common ET severity rating methods is its decoupling from task dependencies. Unlike other measures, which require patients to write, draw, or trace figures like letters or spirals, or perform coordinated tasks with the impaired limb, TETRAS allows for assessment that is decoupled from task-specific performance, which can be easily confounded by deficits in vision, visual-motor coordination and

Table 1.1: TETRAS for Lower Limb ET

Rating	Lower Limb Tremor Amplitude
0	none
1	< 0.5 cm
2	$0.5- < 1$ cm
3	$1- < 5$ cm
4	≥ 5 cm

dexterity [3, 11]. TETRAS thereby provides a substantial improvement on the state-of-the-art by providing a statistically independent measure of ET severity [11].

1.1.1 Tremor Frequency and Analysis

In most cases, the tremor frequency for ET occurs at a frequency band between 4-12 Hz, with more severe ET typically exhibiting a lower frequency range of 4-8 Hz [12, 13, 14]. As previously mentioned, TETRAS classifies the severity of ET based on tremor amplitude-the most common clinical metric for ET-rather than frequency as amplitude of tremor is more strongly correlated with risk of failure and injury in functional tasks [14]. Consequently, TETRAS lacks a distinct evaluation of tremor frequency across different ET severities. Therefore, various ET severities/amplitudes were assigned their corresponding tremor frequencies during simulations by utilizing findings from [12]. It is important to note that TETRAS characterizes tremor for patients with ET only; therefore, the scale does not assess drug induced, rest, or Parkinsonian tremor.

1.1.2 Focusing on Lower Limb Tremor

For this thesis, DNNs will be trained to classify lower-limb tremor based on the lower-limb portion of TETRAS. Table 1.1 presents the amplitudes employed by TETRAS to classify the severity of lower limb tremor, which is assessed bilaterally through heel-shin movement.

To contextualize the findings, ET frequencies were assigned using findings from [12], concerning tremor frequency and its correlation with tremor severity, aligning frequency ranges with TETRAS.

1.2 Issues with TETRAS

However, despite the significant advantages of being well correlated with functional losses and being independent of other common health deficits, TETRAS still exhibits a degree of subjectivity and inconsistency due to potential clinician bias and misdiagnosis. In fact, studies show that up to 10% inter-rater and 5% intra-rater errors have been noted in cumulative ET scores [15]. Additionally, the rate of false positive ET tests, attributed to the poor resolution of common ET severity tests at low tremor levels, has been reported to range between 37%-50% [16, 17]. The low resolution of such assessments is related to the need for such assessments to be manually implementable by a clinician.

Consequently, limitations of existing tremor rating scales, such as TETRAS, are that they require the expertise of a clinician and still result in poor tremor classification. An open problem is the development of a quantifiable, accurate, and repeatable tremor classification scale that can be implemented without trained expertise.

1.3 ET Severity in the Joint Space

Apart from inter- and intra-rater variability, another significant limitation of TETRAS is its low granularity in the joint space. Specifically, TETRAS assumes that ET severity remains constant across all joint angles, which is a notion that is increasingly challenged by recent studies. In fact, numerous clinical studies have noted changes in amplitude and composition of ET from neutral/resting to postured limb positions [18, 19]. As illustrated in Figure 1.1, tremor is often more severe at eccentric angles, where forces such as gravity and joint elasticity impede stabilization (red), compared to stable joint configurations, where inherent dynamics contribute to the stabilization (gray) [20]. More precisely, the position and orientation of the affected limb plays a substantial role in ET movement dynamics. Analysis of these dynamics, which are not included in many common ET assessments, can substantially improve ET diagnosis and treatment. Figure 1.1 superimposes images on our experimental setup to illustrate the disparity in ET severity that results from a joint's stiffness varying with the joint angle. Red indicates more severe ET and occurs where joint stiffness is reduced.

Due to the variations in tremor across the joint space, which is a significant factor in ET severity and is further visualized in Figure 1.2, TETRAS lacks the capability to assist physicians in properly diagnosing and developing effective personalized treatment plans for ET that consider localized factors of the leg contributing the most to the severity of ET, as demonstrated in studies such as [21]. Indeed, TETRAS offers an important tool for approximating quantitative evaluation of ET. However, there remains a clinical need for robust assessment of ET over the joint space. Therefore, as shown in Figure 1.2, a robust ET assessment is proposed that extends TETRAS over the joint space, enabling identification of local and global points of interest in ET affected movement dynamics. To develop this new assessment tool, this thesis leverages machine learning techniques to establish an extension of TETRAS (eTETRAS) to help physicians localize muscles and other biomechanical factors contributing the most to ET severity by assessing the severity of ET across varying joint angles. This approach facilitates the implementation of treatments that require an assessment of tremor severity across the joint space, such as those in [21] and [22], with greater ease and precision. It is important to note that the neutral point depicted in Figure 1.2 is considered as a general reference point when measuring joint angles to show that TETRAS lacks granularity when determining tremor for all limbs. However, for this thesis, the neutral position for the lower limb is defined as when the knee is bent to approximately 90 degrees between the thigh and the shank. Figure 2.1 depicts the reference point (i.e., the neutral position) used in this thesis for measuring knee joint angles.

Figure 1.1: Varying ET Severities Across the Joint Space

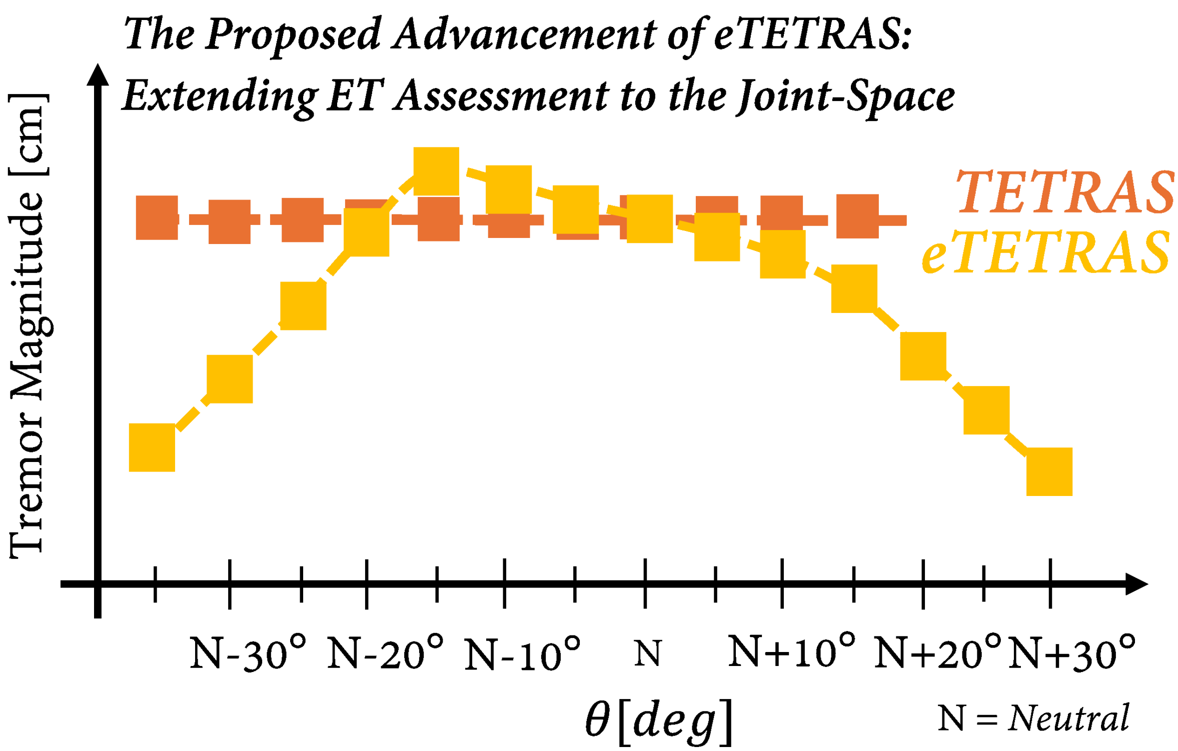

Figure 1.2: The Advancements of eTETRAS Compared to TETRAS

1.4 Time Series Signals and Machine Learning

Quantitative and objective classification of ET, compatible with common scales like TETRAS, can be accomplished using wearable sensors to measure the motion of the affected limbs. The use of wearable sensors, such as inertial measurement units and gyroscopes, have allowed quantitative measurements of ET by converting task specific motion into time-series based signals [23, 24, 25, 26, 27, 28]. Moreover, electromyography sensors can monitors the nerve's stimulation of the muscle to detect tremor activity [29]. These quantitative measurements allow the use of statistics, machine learning, and, due to tremors being quasi-sinusoidal movements, power spectral techniques to aid the diagnosis of ET severity and to help differentiate between Parkinsonian tremor and ET [30, 31, 32, 33, 34, 35, 36]. Driven by the increased attraction and advancements in artificial intelligence (AI), neural networks (NNs) have recently been used to classify and assess tremor severity [35, 36, 37, 38, 39, 40, 41].

These NN-based classifiers employ a variety of NN architectures, including convolutional NNs, artificial NNs, and long short term memory to identify and diagnose various tremors. Most notably, these classifiers utilize affordable and readily available wearable sensors (i.e., accelerometers from smartphones) to collect time-series data for training and classifying tremors with NN's, highlighting the validity and extensive research into the use of wearable sensors and machine learning techniques for tremor classification and its potential application to daily life. Moreover, the increased implementation and improved readiness of AI-driven ET diagnostics can enhance teleoperative approaches in ET diagnosis by enabling individuals with ET to receive treatment and ET diagnosis from the comfort of their homes. As aforementioned, with a steadily aging population and a significant rise in ET cases, the demand for teleoperative approaches in treating ET has reached unprecedented levels. And, with the recent push of AI research, machine learning approaches in tremor medicine show significant promise. However, despite extensive research there is currently no DNN-based approach capable of rapid diagnosis (e.g., 0.5 second increments) of ET severity using TETRAS to the best of the author's knowledge. In this thesis, a multilayer perceptron, that is trained using 0.5 second incremented time series signals obtained from simulations and experiments, is developed to accurately and objectively classify the severity of ET. In addition to eliminating subjectivity during ET severity diagnosis, the results from this thesis will improve the classification of ET before developing an individual's treatment plan. Notably, a distinguishing feature of the developed DNN classifier is its rapid classification ability, with assessments made at 0.5 second intervals. Unlike previous classification methods that analyze tremor severity during post-processing, this rapid approach offers near real-time insights into the variability of tremor during treatments that may require constant monitoring of the severity of tremor [42]. To elaborate, rapid severity diagnosis of ET will provide clinicians with an understanding of the temporal pattern of ET in the context of daily life and activities [42]. Prior classification methods are unable to determine if tremor severity is variable since they analyze tremor severity during post-processing, and a near real-time tremor classification capability can have extensive applications. For instance, near real-time tremor classification can serve as a tool to facilitate novel anti-tremor medications and tremor suppression treatments, and can serve as a categorical factor during a statistical analysis, all of which may need continuous ET severity diagnosis. Furthermore, continuous AI-driven diagnosis can improve teleoperative approaches in both ET diagnosis and treatments requiring ongoing severity assessment.

1.5 Thesis Proposition and Outline

This thesis proposes a novel lower limb ET classifier (eTETRAS) that utilizes a DNN to aid physicians in properly diagnosing ET severity effectively. Unlike conventional classifiers, eTETRAS diagnoses ET rapidly in 0.5 second increments, which enables the continuous assessment of tremor severity. In Chapter 2, an experimental protocol is established, delineating sensor parameters and the testbed used in the generation of a tremor dataset for DNN training and validation. Moreover, this chapter discusses the computer-generated signals used to train the DNN. Chapter 3 presents the first iteration of eTETRAS. In this chapter, the DNN is trained separately with simulated ET knee extension signals and knee encoder measured ET knee extension signals. Chapter 4 expands upon the findings presented in Chapter 3 by proposing a more robust second version of eTETRAS. More specifically, this chapter highlights the joint space parameters, DNN structure, and performance of the second version of eTETRAS. However, unlike the first iteration of eTETRAS, the simulated and experimental datasets are combined to diversify the training set. Moreover, additional performance measures, such as a confusion matrix and F1 scores, are included to assess potential overtraining of the model. The thesis is concluded in Chapter 5 by highlighting the clinical and intellectual contributions of eTETRAS, its limitations, and its future developments.

Chapter 2

Experimental Protocol and Signal Generation

2.1 Experimental Testbed

The lower limb exoskeleton used for this thesis was an Ekso Bionics Indego exoskeleton as depicted in Figure 2.1. An optical encoder, located at the knee, measured the angular displacement between the vertical axis and the shank as depicted in Figure 2.1 as θ.

2.2 Participants

A single able body subject (23 year old male) participated in this pilot study. Prior to participation, written informed consent was obtained from the participant, as approved by the institutional review board at Auburn University. The exoskeleton testbed IRB number is 23-100 MR 2303.

2.3 Experimental Protocol

The participant was asked to extend their knee to near full extension over a duration of approximately 2.5 seconds and to flex their knee back to the initial position over another duration of approximately 2.5 seconds for a knee extension and flexion frequency of 0.2 Hz. The total experimental run time was 200 seconds, which led to approximately 40 leg extension repetitions. To simulate a tremor, a sinusoidal input with an amplitude and frequency obtained from the TETRAS scale and [12] was injected into the motor at the knee. The motor input that was designed to represent tremor was recorded by the control software. An optical encoder measured the angle of the knee during knee extension and flexion and captured the knee angle measurements at 200 Hz. The encoder measurements

Figure 2.1: Exoskeleton Testbed

were separated into 0.5 second intervals in real-time for a total of 101 sample per training feature. These segmented encoder measurements were then used to train and test a DNN.

2.4 Signal Generation for Simulation

In MATLAB, a dataset comprising of 25,000 leg extension signals was generated for training a single DNN. Being that this thesis primarily focuses on ET in the lower limb during leg extensions, each signal represents knee angle measurements between the vertical axis and the shank of the leg, as illustrated in Figure 2.1. These signals are sinusoidal with a frequency of 0.2 Hz and maximum/minimum angles of 70 degrees and 0 degrees, respectively. To ensure rapid DNN response and to mimic the sampling frequency of the exoskeleton testbed in Figure 1, each signal had a sampling frequency of 200 Hz over a 0.5 second interval, resulting in a total of 101 samples per signal. Additionally, an auxiliary ET signal was incorporated into the aforementioned signals to simulate ET during leg extensions. The ET signals followed a sinusoidal trajectory, and are scaled based on the severity criteria outlined in Table 1.1. To account for the frequencies associated with different ET severities, ET signals with greater amplitudes (indicating more severe ET) were given lower frequencies, consistent with the findings in [12]. The generated signals, denoted as $\phi \in \mathbb{R}^{101}$, are defined as

$$\phi_i = (35 - 35\cos(P + 0.4\pi t_i)) + \sin^{-1}\left(\frac{A\sin(2\pi\sigma t_i)}{2L}\right) \tag{2.1}$$

where ϕ_i is the i^{th} element of ϕ, $i \in \mathbb{Z}$ takes values from 0 to 100, $t_i = 0.005i$ is the time index that ranges from 0 and 0.5 seconds, $P \in \mathbb{R}_{\geq 0}$ is the phase of the signal which has a value randomly selected from 0 to 2π such that $P \in [0, 2\pi]$, $A \in \mathbb{R}$ is the amplitude associated with the ET signal, randomly selected based on the criteria in TETRAS, $\sigma \in \mathbb{R}$ denotes the frequency of the ET signal, selected based on the randomly selected tremor amplitude, and $L \in \mathbb{R}$ is the length of the leg. Subsequently, the signals were labeled based on the severity of the tremor to represent the true tremor classification.

Chapter 3

First Iteration of eTETRAS

3.1 Neural Network Structure and Training of eTETRAS Version 1

Figure 3.1 depicts the DNN architecture used to classify ET in this thesis. The DNN structure is a multi-layer perceptron with three hidden layers that takes the knee angle measurements as the DNN inputs.

Weights and biases are implemented at each layer of the DNN, where the outputs of the hidden layers are fed into rectified linear activation function. Each hidden layer contained 15 neurons, a Rectified Linear Unit (ReLU) activation function, and were connected to the next layer. To compute the confidence and classify the severity of the ET, the outputs of the output-layer vector had 4 elements that were fed into a softmax activation function. The DNN $f : \mathbb{R}^{101} \rightarrow \mathbb{R}^4$ can be defined as

$$f = \sigma_4 \left(W_4 \sigma_3 \left(W_3 \sigma_2 \left(W_2 \sigma_1 \left(W_1 x + b_1 \right) + b_2 \right) + b_3 \right) + b_4 \right) \tag{3.1}$$

where $\sigma_4 : \mathbb{R}^4 \rightarrow \mathbb{R}^4$ is the activation function associated with the output layer, $W_4 \in \mathbb{R}^{4\times 15}$ are the output layer weights, $b_4 \in \mathbb{R}^4$ are the output layer biases, $W_3, W_2 \in \mathbb{R}^{15\times 15}$ are the hidden layer weights, $b_3, b_2 \in \mathbb{R}^{15}$ are the hidden layer biases, $\sigma_3, \sigma_2, \sigma_1 : \mathbb{R}^{15} \rightarrow \mathbb{R}^{15}$ are the hidden layer activation functions, $W_1 \in \mathbb{R}^{15\times 101}$ is the input layer weights, $b_1 \in \mathbb{R}^{15}$ is the input layer biases, and $x \in \mathbb{R}^{101}$ is a vector of inputs of the DNN which are the knee angle measurements. The value of each element in the output layer ranges from 0 to 1 and corresponds to the severity of the ET. To be specific, the first element of the vector indicates level 0-1 ET severity while the final element indicates level 4 ET severity according to TETRAS. The element with the greatest value indicates the severity of the

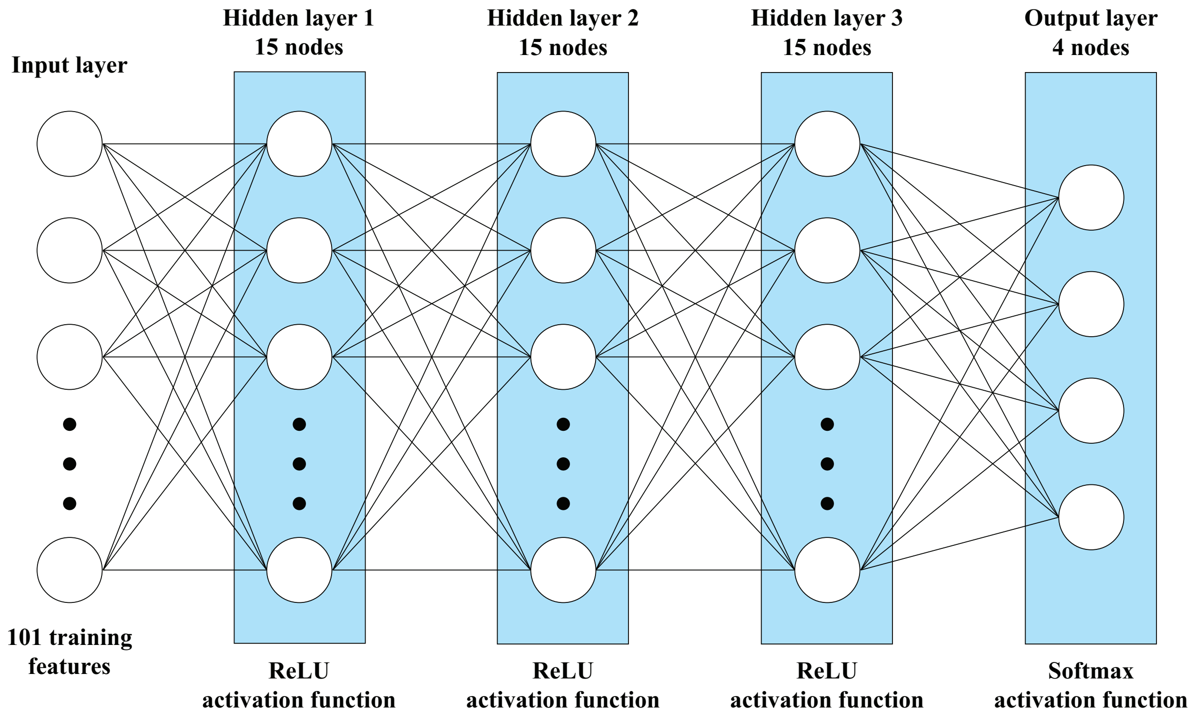

Figure 3.1: Version 1 eTETRAS 1-Dimensional DNN Structure

ET. Categorical cross-entropy was selected as the loss function for the DNN, and the Adam optimizer algorithm was used to train the DNN. A total of 300 epochs and a batch size of 101 was selected to train the DNN using the simulation data. For the experimental data, a batch size of 70 was used, instead. To monitor the performance and prevent over-fitting, the data was randomly split where 75% of the training data was used to train the DNN, while the remaining 25% of the data was used to validate the DNN.

3.2 Evaluation of eTETRAS Version 1

As aforementioned, the purpose of this thesis is to classify the severity of ET rapidly (i.e., 0.5 second increments) using a multi-layered perceptron.

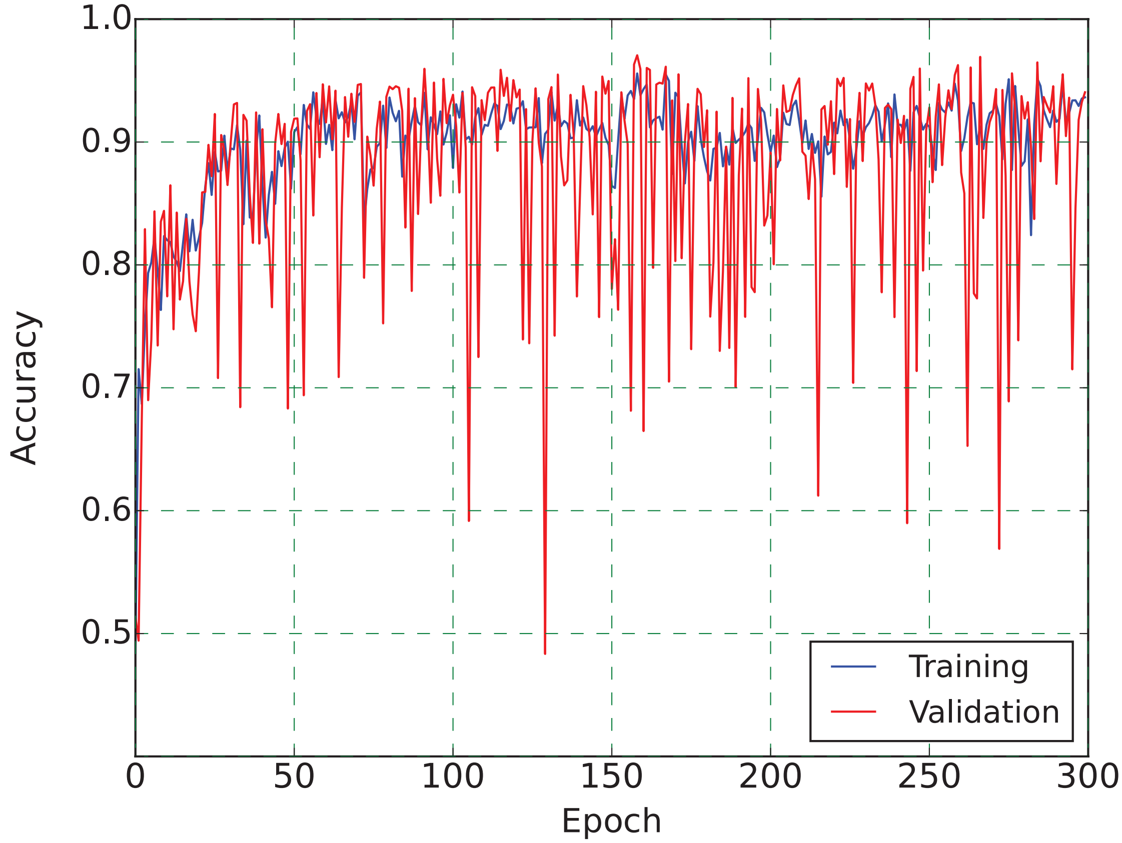

Figure 3.2: Simulated Signals Training and Validation Accuracy of eTETRAS Version 1

3.2.1 Simulation Results

Knee angle measurements that were created and ranked using criteria outline from TETRAS was used to train the DNN. Figure 3.2 depicts the training and validation accuray of the DNN per training epoch. After 300 training iterations, the model achieved 93.63% training accuracy and 94.05% validation accuracy. Moreover, referencing Figure 3.2, the blue and red lines indicate the training and validation accuracy per epoch, respectively.

3.2.2 Experimental Results

To validate the effectiveness of implementing a DNN to classify the severity of ET, shank-angle measurements were taken from an encoder located at the knee of the exoskeleton testbed, all from the same participant from the first iteration of eTETRAS. A artificial tremor was injected into the knee motor of the exoskeleton and ranked using the TETRAS scale.

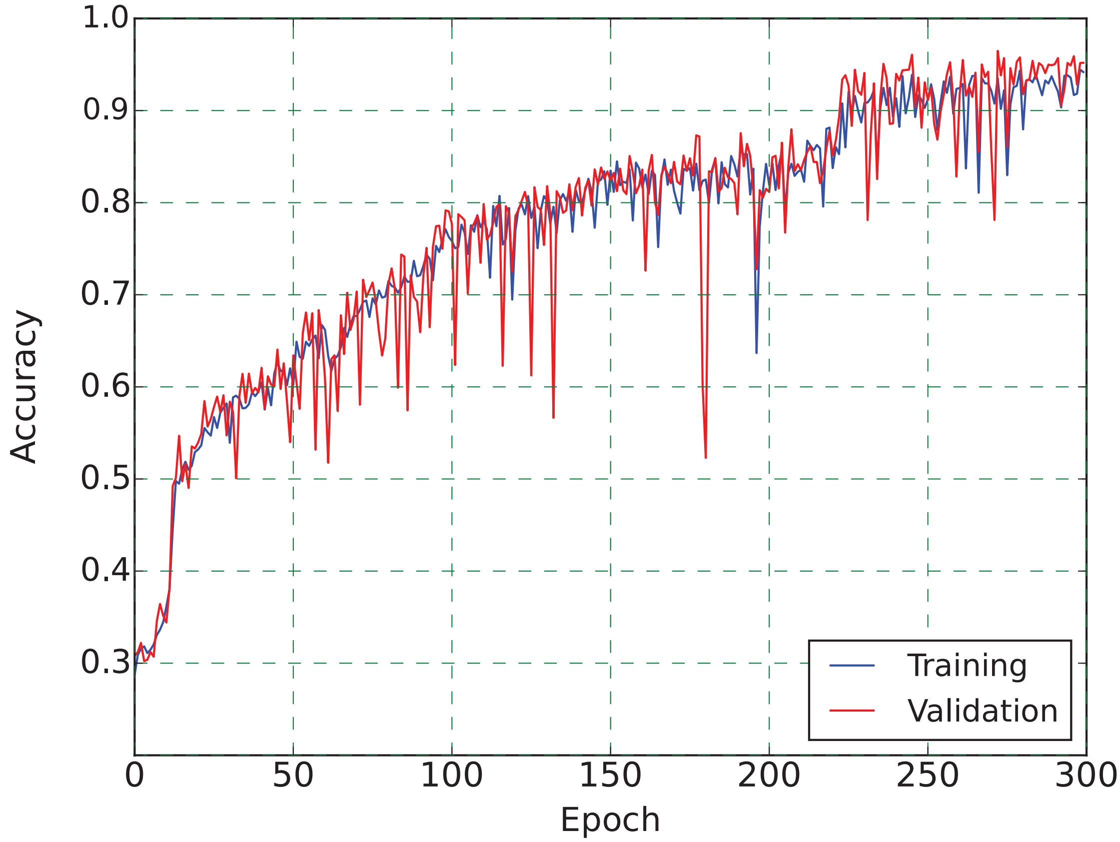

Figure 3.3: Experimental Signals Training and Validation Accuracy of eTETRAS Version 1

Figure 3.3 depicts the training and validation accuracy of the DNN per training epoch. After 300 training iterations, the model achieved a 94.80% training accuracy and a 95.18% validation accuracy.

3.3 Discussion of eTETRAS Version 1

The proposed DNN structure has been proven to be effective in classifying the severity of ET. That is, the simulation results indicate a 93.63% training accuracy, and the experimental results indicate a 94.80% accuracy. In subsequent chapters, a more diverse training dataset will be created by synthesizing and randomizing the experimental and simulation based datasets. To be specific, since two separate DNNs were trained using a simulated and experimental datasets, combining the MATLAB generated signals with the encoder measurements could further diversify the dataset. This approach will ensure that the DNN-based classifier captures various features within the training set, which ultimately improves the generalizability of eTETRAS.

It should be mentioned that the DNN exhibited better performance (i.e., training accuracy and validation) when the experimental signals generated from the optical encoder were inputted into the DNN. Despite potential noise and biases introduced by sensor measurements, this improvement in performance may be credited to the post-processing techniques (e.g., signal filtering) applied to the sensor data prior to inputting it into the DNN. In actuality, research has indicated that the DNN's performance is influenced by signal characteristics used for training [43, 44]. Consequently, the DNN demonstrated improved performance due to the application of a zero order hold on the knee encoder which, in turn, introduced discretized sensor data to the input of the DNN.

It is important to note that while tremors are characterized as sinusoidal oscillations in this pilot study, research suggests that ET signals exhibit asymmetric, quasi-sinusoidal patterns [45, 46]. This asymmetry can be attributed to various factors in the leg, such as differing joint stiffness across the joint space and the viscoelastic effects of the leg. This can be addressed by leveraging the generalizability of DNNs as the quasi-sinusoidal features may be captured in the experimental data. Moreover, the use of half-second increments might not provide sufficient time for the asymmetric tremor behavior to be expressed within the signal, which may result in a more sinusoidal pattern for each training feature. Nonetheless, future efforts will incorporate the varying parameters of the leg as inputs, such as joint stiffness, enhancing the categorical performance of the DNN.

Chapter 4

Second Iteration of eTETRAS

4.1 Robust Joint Space Model with Stochastic Calculus

The tremor spatiotemporal characteristics at the knee vary continuously with joint angle, instantaneous rotational moment of inertia, joint stiffness, and viscous musculotendinous dynamics at the knee. As shown in [47] and [48], the angle of the knee joint can be mathematically expressed with a differential equation defined as

$$M_I(\ddot{\theta}) + M_v(\dot{\theta}) + M_e(\theta) + M_g(\theta) = \tau_{vol} + \tau_T, \tag{4.1}$$

where $M_I \in \mathbb{R}$ denotes the inertia of the lower limb, $M_e \in \mathbb{R}$ is the elastic effects at the knee induced by joint stiffness, $M_g \in \mathbb{R}$ denotes a torque due to gravity, $M_v \in \mathbb{R}$ denotes the viscous damping effects at the knee, $\tau_{vol} \in \mathbb{R}$ denotes the volitional torque produced by the user about the knee joint, and $\tau_T \in \mathbb{R}$ denotes the torque produced by tremor. The inertial and gravitational effects in equation 4.1 can be modeled as

$$M_I = I\ddot{\theta}, \quad M_g = mgl\sin(\theta), \tag{4.2}$$

where $\theta \in \mathbb{R}$ denotes the measured, twice differentiable knee angle, I, m, $l \in \mathbb{R}_{>0}$ are parameters of the leg and $g \in \mathbb{R}_{>0}$ is the gravitational constant.

As shown in [49] and [47], the elastic and viscous effects about the knee can be defined as

$$M_e = k_1(\exp(-k_2\theta))(\theta - k_3), \tag{4.3}$$

$$M_v = -B_1\tanh\left(-B_2\dot{\theta}\right) + B_3\dot{\theta}, \tag{4.4}$$

where k_1, k_2, $k_3 \in \mathbb{R}_{\geq 0}$ are uncertain parameters associated with the elastic effects, and B_1, B_2, $B_3 \in \mathbb{R}_{\geq 0}$ are uncertain parameters associated with the viscous damping effects of the leg.

To guarantee accurate modeling of tremor severity in practical timescales, the input space of the machine learning model must be a robust Markov representation of the dynamic space [50, 51]. Therefore, the input space must encompass the position state θ, which is the input space of the classical TETRAS and the eTETRAS presented in Chapter 3, and the joint stiffness, which is in the expanded input space constituting the novel contribution of eTETRAS in this chapter. This inclusion allows for the interpretation of tremor variability across the continuous joint space. However, accurately computing the unmeasured states $\dot{\theta}$ and $\ddot{\theta}$ from θ using the mathematical model in equation 4.1 is challenging, especially in the presence of nonlinearities and uncertain parameters. Additionally, numerically or analytically obtaining the first and second time derivative from position alone is time-consuming and can impede practical online learning [52].

The complexity of the dynamics in equation 4.1 motivate the development of a general Markov input space, and correspondingly, the wearable sensing strategy. It will be demonstrated that the dynamics in equation 4.1 can be approximated as dependent only on θ and the standard deviation of θ, which is computationally less expensive to obtain than time derivatives.

First, it is assumed that θ, $\dot{\theta}$, and $\ddot{\theta}$ have continuous probability density functions, θ is locally stationary and ergodic within sliding epochs in which oscillations like those characteristic of tremor are relatively small in amplitude, the global trajectories of θ and its derivatives are continuous, smooth, and differentiable, and the sampling rate is stable [53]. Then, utilizing the definition of variance, a relationship is established between the variance of θ and the integral of the variance of its derivative, which is defined as

$$\begin{aligned}\mathrm{Var}(\theta) &= \mathbb{E}\left[\left(\int_0^T \dot{\theta}(t)dt - \mathbb{E}\left[\int_0^T \dot{\theta}(t)dt\right]\right)^2\right] \\ &= \mathbb{E}\left[\left(\int_0^T \left(\dot{\theta}(t) - \bar{\dot{\theta}}\right) dt\right)^2\right] \\ &= \int_0^T \mathrm{Var}(\dot{\theta}(t))dt,\end{aligned} \tag{4.5}$$

where $\mathrm{Var}(\cdot)$ is the variance of $(\cdot)$, $\mathbb{E}[\cdot]$ is the expected value of $[\cdot]$, and $\mathrm{T} \in \mathbb{R}$ is the sliding epoch length. Next, using the definitions of the standard deviation and variance, an approximate relationship between the standard deviation of θ and the integral of the variance of its derivative is established:

$$\mathrm{std}(\theta) \approx \sqrt{\int_0^T (\theta(t) - \bar{\theta})^2 dt} \approx \sqrt{\int_0^T \mathrm{Var}(\dot{\theta}(t))dt}, \tag{4.6}$$

and by the definitions of standard deviation and variance, it follows that $\mathrm{std}(\theta) \approx \mathrm{std}(\dot{\theta})$. Under the given assumptions, it is important to note that when $\mathrm{Var}(\ddot{\theta}) = \int_0^T \mathrm{Var}(\frac{d\theta}{dt}(t))dt$ is considered, then $\mathrm{std}(\theta) \approx \sqrt{\int_0^T \mathrm{Var}(\ddot{\theta}(t))dt} = \mathrm{std}(\ddot{\theta})$, which is indicative of the sinusoidal time-frequency regularity of tremor. It is also worth noting that standard deviation quantifies the variability of theta within the epoch. Specifically, greater values of $\dot{\theta}$ correlates to a greater standard deviation of θ, especially for local stationary sinusoidal signals like tremor. Leveraging these definitions to construct finite-difference based approximations and noting that the sampling time and sliding window Δt were treated as fixed constants, the states $\dot{\theta}$ and $\ddot{\theta}$ can be approximated as

$$\begin{aligned}\ddot{\theta} &\approx \frac{\Delta\dot{\theta}}{\Delta t} \approx \frac{\sqrt{\int_0^T \mathrm{Var}(\dot{\theta}(t))dt}}{\Delta t} = \frac{\mathrm{std}(\dot{\theta})}{\Delta t} \approx \frac{\mathrm{std}(\theta)}{\Delta t} \\ \dot{\theta} &\approx \frac{\Delta\theta}{\Delta t} \approx \frac{\sqrt{\int_0^T \mathrm{Var}(\theta(t))dt}}{\Delta t} \approx \frac{\mathrm{std}(\theta)}{\Delta t}.\end{aligned} \tag{4.7}$$

Therefore, it can be shown that a robust dynamic input space represented with θ and std(θ) can be approximated, given the sinusoidal regularity of tremor and knee flexion/extension, and with sufficient statistical conditions. The constant time difference and other parameters of the model can be approximated by scaling and bias layers in classical machine learning models. Consequently, the input to the model in (4.1) can be approximated as $[\theta \quad \text{std}(\theta)]^T$.

$$\begin{aligned} & M_I(\ddot{\theta}) + M_v(\dot{\theta}) + M_e(\theta) + M_g(\theta) \\ \approx & M_I(std(\theta)) + M_v(std(\theta)) + M_e(\theta) + M_g(\theta) \end{aligned} \tag{4.8}$$

Thus, with expressions for $\dot{\theta}$ and $\ddot{\theta}$ with respect to θ and std(θ), the DNN has a low-dimensional, computationally inexpensive Markov input space from which to estimate $[M_I + M_e + M_g + M_v]|_\theta$ toward understanding the comprehensive system behavior online for robust predictions in the joint space. The avoidance of computing derivatives leads to significantly faster inference times and streamlined model training. In (4.7), it is worth noting that the frequencies of angular acceleration, velocity, and position are sinusoidal signals, and their time derivative frequencies remain similar to one another. Only the phase changes, which are neglected in this analysis, contribute to the differences.

4.2 Neural Network Structure and Training of eTETRAS Version 2

Figure 4.1 depicts the DNN architecture used to classify ET in this work. The DNN structure is a multi-layer perceptron with six hidden layers that takes the knee angle measurements and their standard deviation as the DNN inputs. The first three hidden-layers consist of a 3-D DNN architecture, where each layer is sequentially connected but operate independently without direct connections to each other. Subsequently, the outputs of these layers are combined and flattened with the concatenate layer, then fed into the sequentially connected 1-D set of layers. Weights and biases are implemented at each layer of the DNN,

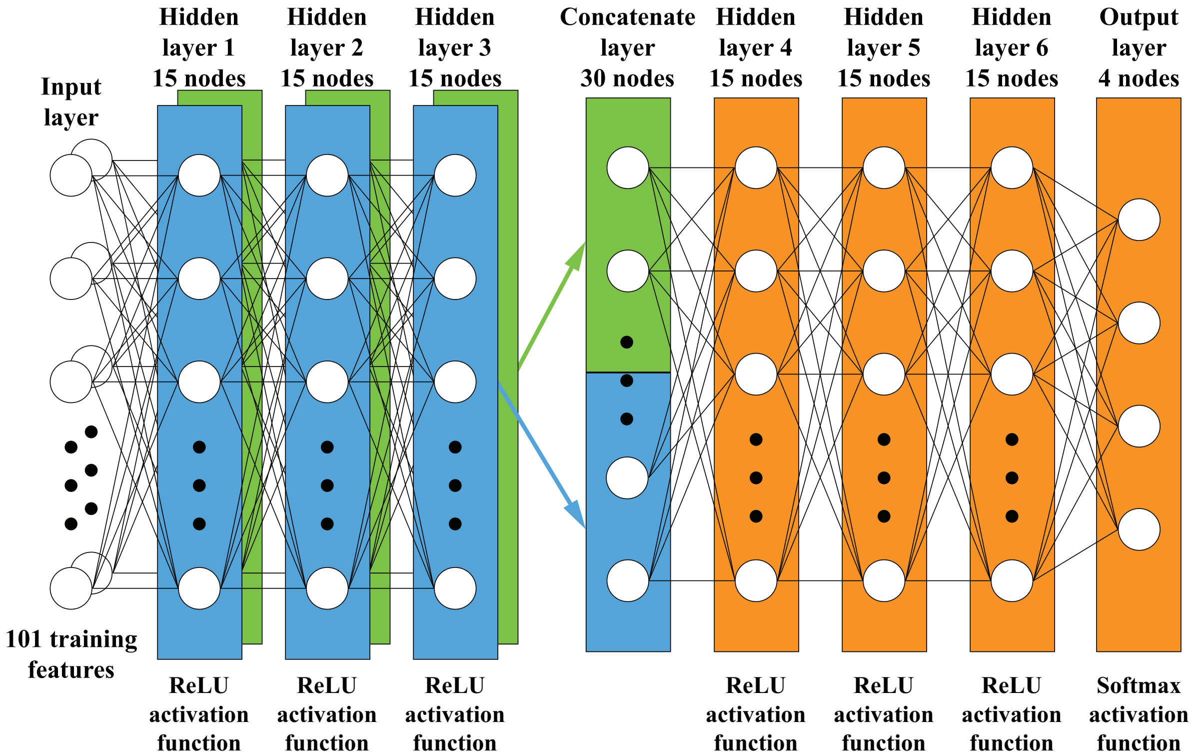

Figure 4.1: Version 2 eTETRAS 2-Dimensional DNN Structure

where the outputs of each hidden layers, other than the concatenate layer, are fed into rectified linear activation functions. Each hidden layer contained 15 neurons each. To compute the confidence and classify the severity of the ET, the outputs of the output-layer vector had 4 elements that were fed into a softmax activation function. The value of each element in the output layer ranges from 0 to 1 and corresponds to the severity of the ET. To be specific, the first element of the vector indicates level 0-1 ET severity while the final element indicates level 4 ET severity. The element with the greatest value indicates the severity of the ET. Categorical cross-entropy was selected as the loss function, and the Adam optimizer algorithm was used to train the DNN. A total of 200 epochs and a batch size of 200 was selected to train the DNN for all datasets. To monitor the performance and prevent over-fitting, the data was randomly split where 75% of the training data was used to train the DNN, while the remaining 25% of the data was used to validate the DNN.

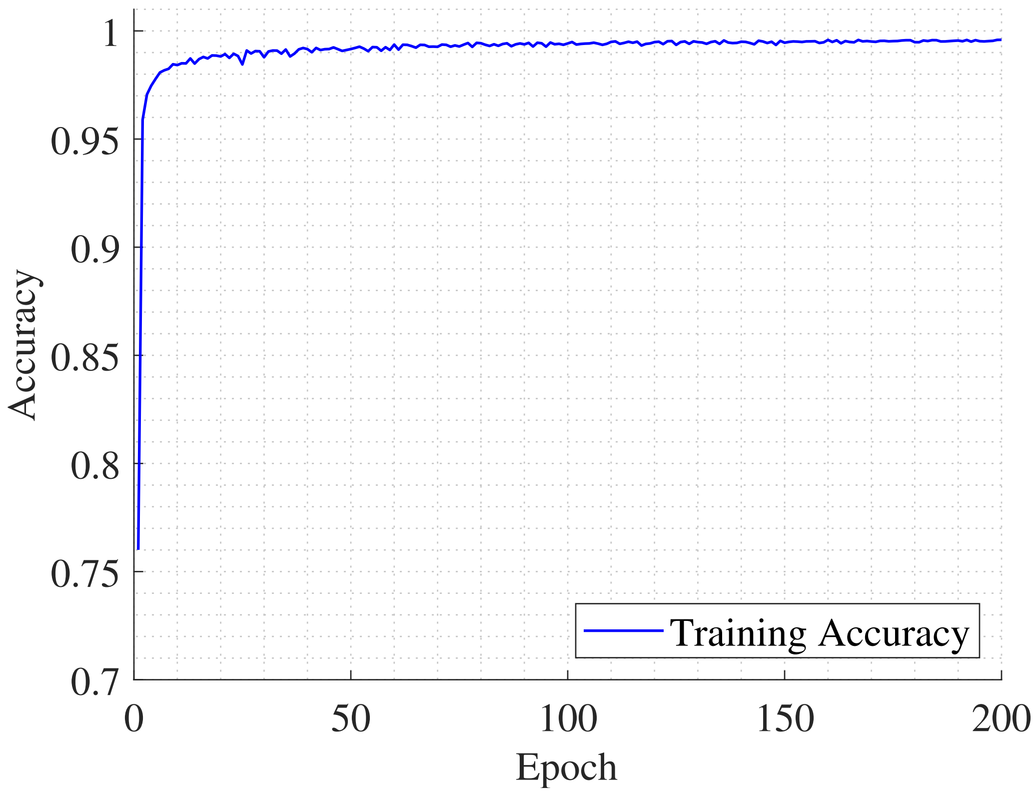

Figure 4.2: Training Performance per Epoch of Simulation-based DNN

4.3 Evaluation of the Deep Neural Network

As previously mentioned, the purpose of this pilot study is to classify the severity of ET in real-time using a multi-layer perceptron. Results from the simulation, and the initial pilot study demonstrate the feasibility of this approach.

4.3.1 Simulation Results

Knee angle measurements that were created and ranked using the criteria obtained from the TETRAS scale was used to train the DNN. Figure 4.2 depicts the training accuracy of the DNN per training epoch. After 200 training iterations, the model achieved a 99.59% training accuracy.

To further illustrate the performance of the DNN trained via simulation data, Figure 4.3 depicts the confusion matrix for the simulated DNN-based eTETRAS classifier. This matrix

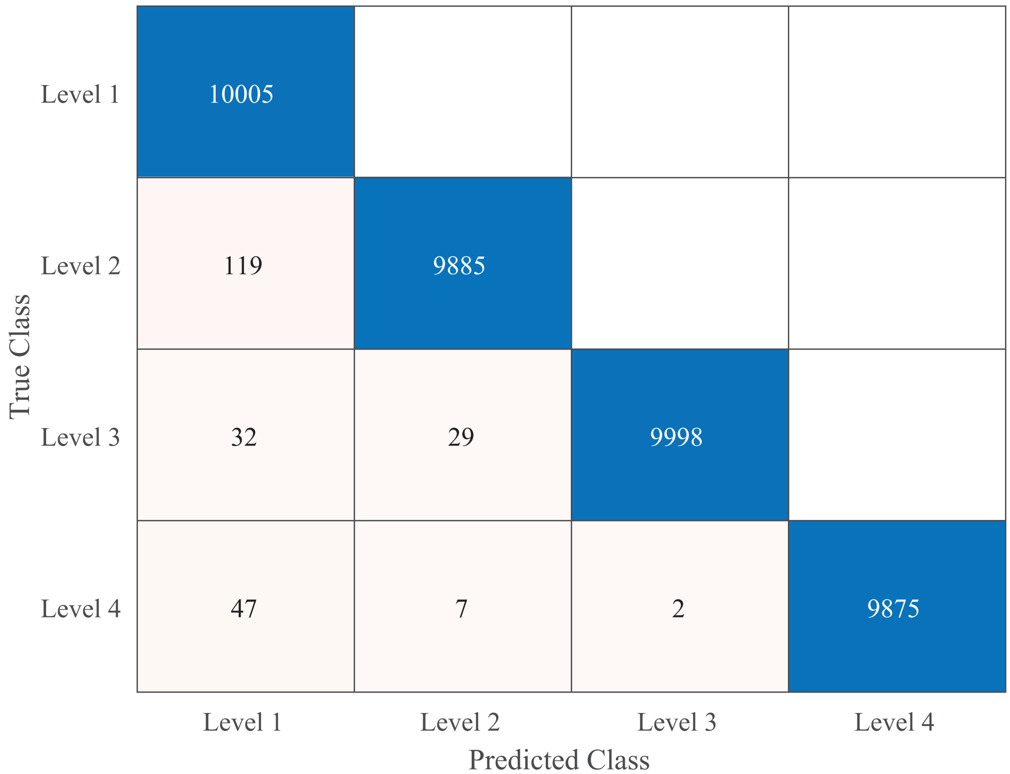

Figure 4.3: Confusion Matrix of the Simulation-based DNN

Table 4.1: F1 Scores of the Simulation-based DNN

Tremor severity	Precision	Recall	F1-Score
Level 1	0.9806	1.0000	0.9902
Level 2	0.9964	0.9881	0.9922
Level 3	0.9998	0.9939	0.9969
Level 4	1.0000	0.9944	0.9972

represents how the validation dataset performed when tested on the DNN. The confusion matrix aids in identifying the classes where the eTETRAS classifier is incorrectly classifying and indicates if the model is over-trained.

Referring to Figure 4.3, it can be observed that most of the confusion occurs between the level 1 and level 2 tremor severity classes. This may be attributed to the similarity between level 1 and level 2 tremors, causing confusion for the DNN. Similar trends can be observed for other classes as well; for instance, there is some confusion between the level 2 and level 3 tremor severity classes. For a more comprehensive view of misclassifications, Table 4.1 presents the precision, recall, and F1 score performance for each element class.

Referencing Table 4.1, it can be observed that missclassifications of level 1 severity tremors were most often due to missclassifying a tremor as a false level 1 severity tremor. This can be observed by the higher recall score but lower precision score for this class, indicating that while the model frequently identifies true level 1 tremors, it also incorrectly identifies non-level 1 tremors as level 1. This finding aligns with the findings presented in Figure 4.3 and is reflected in the lower F1-score. Conversely, the model tends to missclassify level 3 tremors as false level 2 tremors, as evidenced by a lower precision score but a greater recall score.

4.3.2 Experiment Results

To validate the effectiveness of implementing a Deep Neural Network (DNN) for classifying the severity of ET, shank-angle measurements were taken from the same participant during the initial eTETRAS iteration. Similar to the first iteration, these shank-angle measurements were obtained from an encoder situated at the knee of the exoskeleton testbed. An artificial tremor was injected into the knee motor of the exoskeleton and ranked using the TETRAS scale. Figure 4.4 depicts the training accuracy of the DNN per training epoch. After 200 training iterations, the model achieved a 100% training accuracy. To further explore the performance of the experimental-based DNN, Figure 4.5 depicts the confusion matrix for the experimental-based DNN classifier wherein the validation dataset was tested on the DNN.

Referencing Figure 4.5, it can be observed that only minor missclassification occurs between the classes. To further illustrate the performance of the DNN, Table 4.2 presents the recall, precision and the F1 score performance of the experimentally trained DNN wherein the validation dataset was tested on the DNN.

From Table 4.2, it is important to note the lower recall and precision scores for the level 4 class. This could be attributed to the minimal missclassification of level 4 tremors into

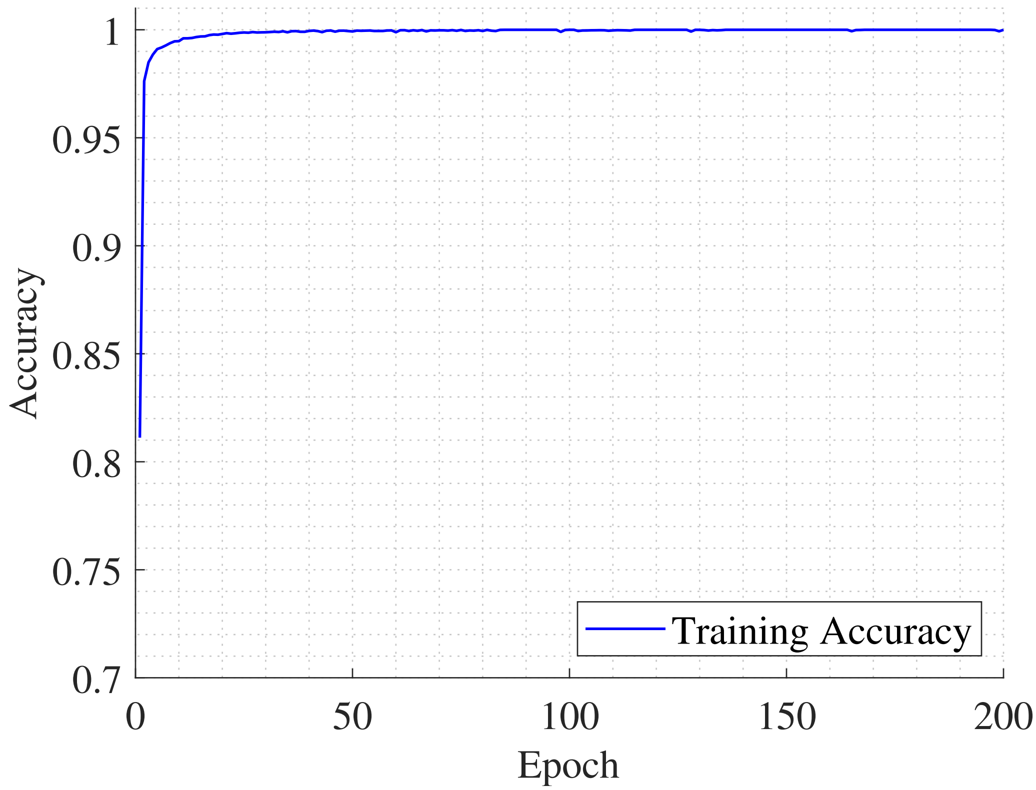

Figure 4.4: Training Performance per Epoch of Experimental-based DNN

Table 4.2: F1 Scores for the Experimental-based DNN

Tremor Severity	Precision	Recall	F1-Score
Level 1	1.0000	1.0000	1.0000
Level 2	0.9999	1.0000	0.9999
Level 3	1.0000	1.0000	1.0000
Level 4	1.0000	0.9999	0.9999

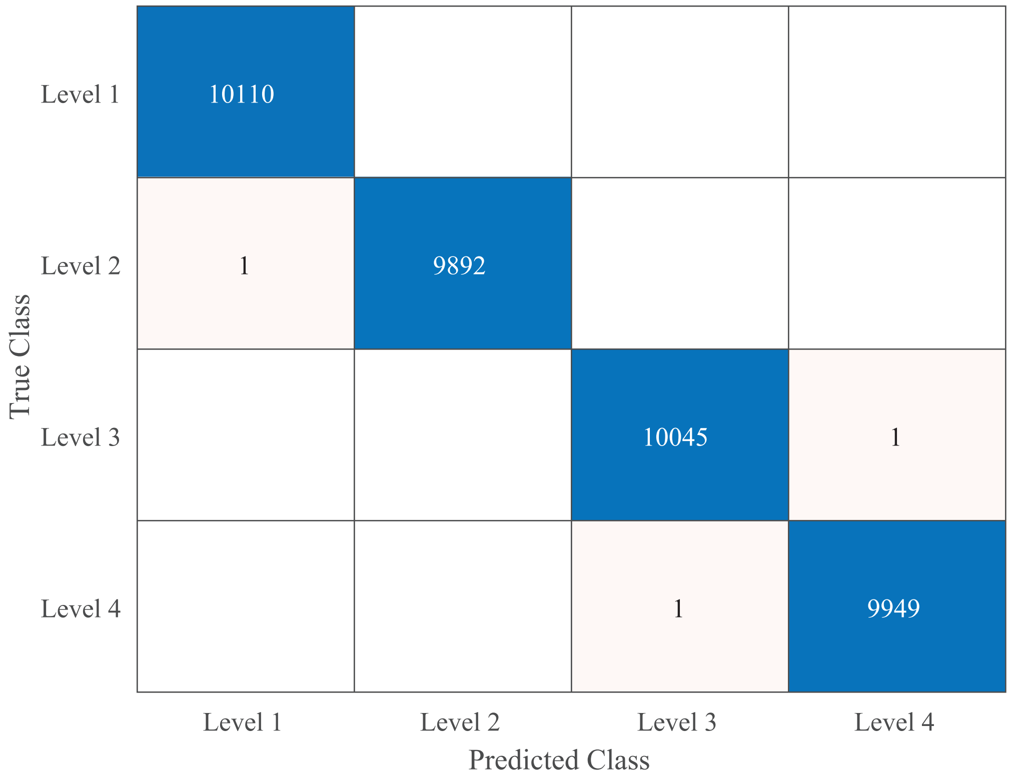

Figure 4.5: Confusion Matrix of the Experimental-based DNN

other classes. Notably, the highest frequency of missclassification occurs between the level 3 and level 4 tremor severities; however, these errors are negligible.

4.3.3 Combining Experimental and Simulated Data

It is important to note that the two data-sets separately may be insufficient in size, potentially leading to over fitting of the DNN and reducing its generalizability. To address this limitation, the experimental and simulated tremor data were synthesized and randomly mixed, to diversify and expand the data-set. Figure 4.6 depicts the training accuracy of the eTETRAS classifier. After 200 epochs, the eTETRAS classifier achieved a training accuracy of 99.65%.

Referencing the confusion matrix illustrated in Figure 4.7, the eTETRAS classifier exhibits behavior similar to that of the simulated DNN. Specifically, the eTETRAS classifier

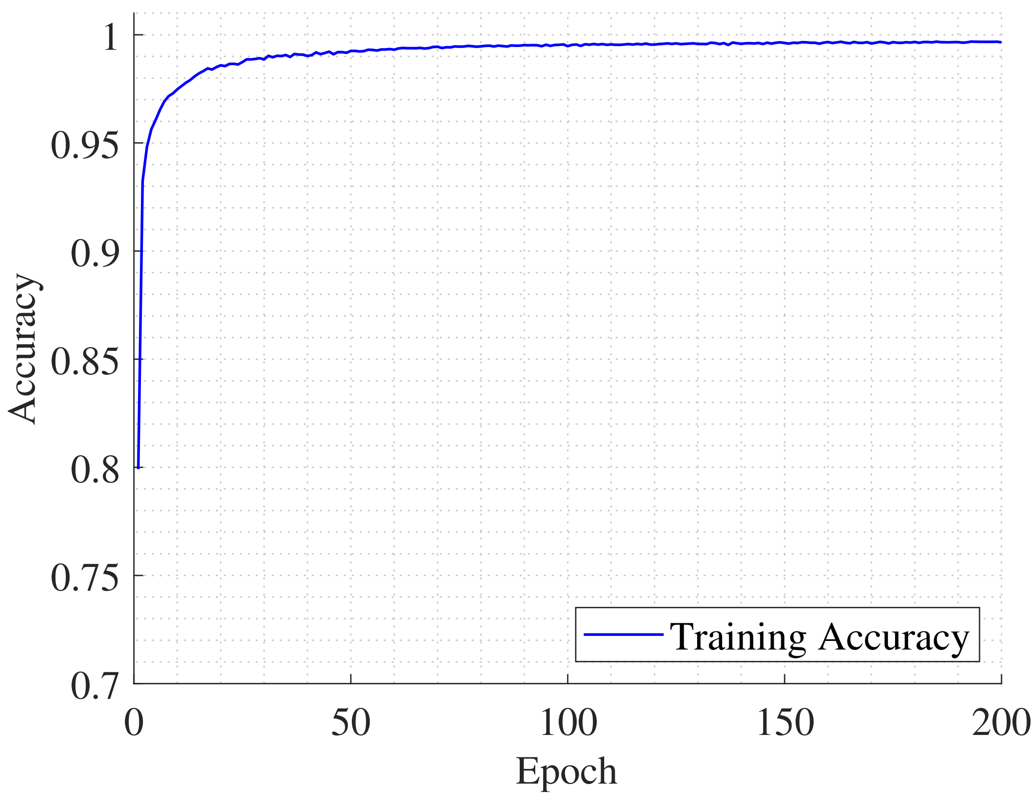

Figure 4.6: Training Performance per Epoch Using Combined Dataset

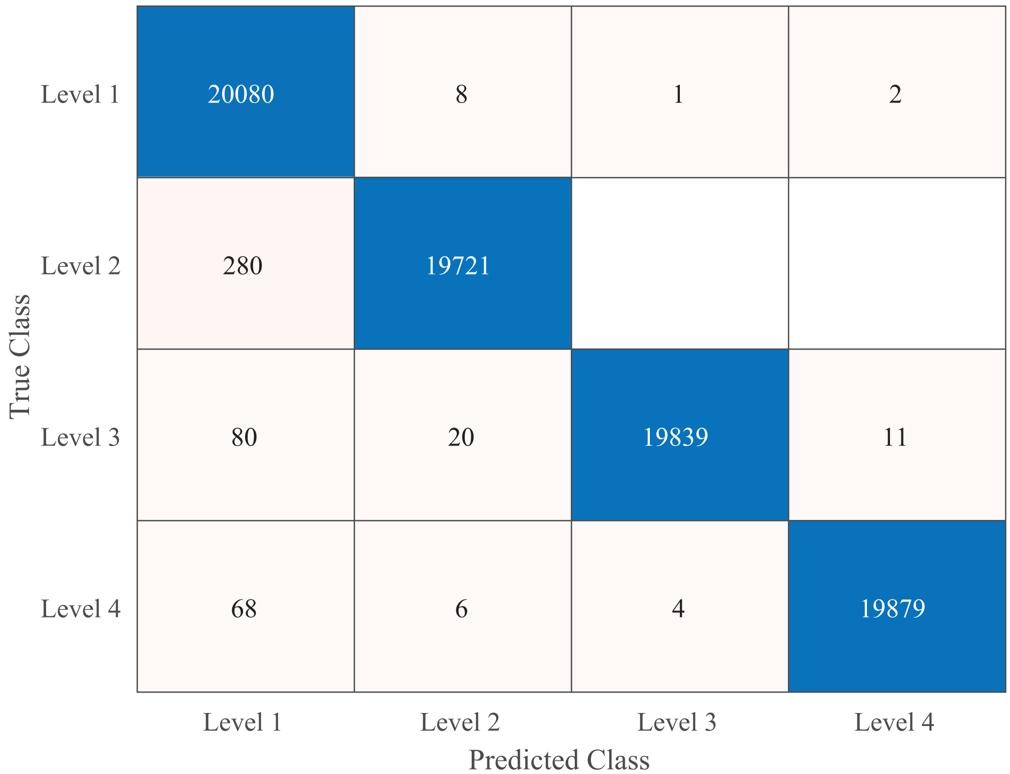

Figure 4.7: Confusion Matrix Using the Combined Dataset

Table 4.3: F1 Scores for the Combined dataset DNN

Tremor severity	Precision	Recall	F1 Score
Level 1	0.9791	0.9995	0.9892
Level 2	0.9983	0.9860	0.9921
Level 3	0.9997	0.9944	0.9971
Level 4	0.9993	0.9961	0.9977

tends to missclassify tremors that are level 2 in severity as level 1 severity. For a more comprehensive view of the eTETRAS classifier performance, Table 4.3 presents the precision, recall and F1 Scores of eTETRAS.

From Table 4.3, it is evident that the eTETRAS classifier performs well in correctly identifying level 1 tremors, as indicated from the greater recall score corresponding to the level 1 category. However, the lower precision score indicates that the eTETRAS classifier has a tendency to missclassify other level tremors as level 1, lowering the precision score to 0.9791. This means that the classifier accurately predicted 97.91% of level 1 tremors as level 1. Consistent with the findings from the confusion matrix, the eTETRAS classifier often missclassifies level 2 tremor as level 1 tremor. This finding can be supported with the lower recall score associated with the level 2 tremor class, indicating that 98.60% of level 2 tremors were correctly predicted out of all true level 2 tremors.

4.4 Discussion of eTETRAS Version 2

The proposed eTETRAS has been proven to be effective in classifying the severity of ET. That is, the simulation results indicate a 99.59% training accuracy, the experimental results indicate a 100% accuracy, and the combined results indicate a 99.65% training accuracy.

It is important to highlight that the DNN achieved better training accuracy with the experimental and combined dataset similarly to the first iteration of eTETRAS. This improvement could be attributed to the filtering applied to the optical encoder and the variable frequency involved during leg extension and flexion motions. To elaborate, the rate of the experimental knee flexion and extension motions may not precisely have been at 0.2 Hz; instead, it fluctuates around a neighborhood of 0.2 Hz. This variability in knee flexion and extension may potentially diversify the training set, thereby enhancing the training and validation accuracy of the DNN. Additionally, the performance of the DNN is influenced by the characteristics of the signals that are used to train the DNN [43, 44]. The application of a zero order hold to the knee encoder measurements introduced discretized sensor data to the training set, potentially influencing the training performance of the DNN.

It is noteworthy that the eTETRAS classifier encountered challenges in accurately classifying level 2 tremors, often misdiagnosing them as level 1 severity. This issue arises from the similarity between the signals of level 1 and level 2 tremors, leading to confusion and misclassification by eTETRAS. As per the criteria outlined in Table 1.1, both level 1 and level 2 tremors exhibit closely aligned tremor amplitudes, with level 1 tremors falling below 0.5 cm and level 2 tremors ranging from 0.5 to less than 1 cm. This similarity is reflected in the lower F1-scores associated with these respective classes. Conversely, level 3 and level 4 tremor severities exhibit a wider range of amplitudes, with level 3 tremor amplitudes ranging from 1-5 cm and level 4 tremor ranging $\geq$5 cm. Consequently, eTETRAS can distinguish between level 3 and level 4 tremors more effectively. It is also crucial to acknowledge that tremors lying in the transition zones, such as tremors with amplitudes of 0.49, which closely resembles level 2 tremor, may lead to misclassifications by eTETRAS due to the inherent similarity with neighboring levels. This limitation hinders the recall, precision, and F1-Scores from achieving maximum values of 1.

Chapter 5

Conclusion

ET is the most common type of movement disorder that causes tremor, characterized by rhythmic and involuntary shaking of an individual's limbs during task specific actions. As it stands, the diagnosis of ET severity relies on highly subjective and inconsistent methods, leading to clinical errors such as bias from inter- and intra- rater errors. These errors are caused, by but not limited, to inconsistent measurement techniques amongst clinicians due to the lack of stringent diagnostic criteria, systematic thinking errors, and measurement errors [54]. This thesis marks the initial phase in the creation of an AI driven tremor classification system capable of diagnosing the severity of ET continuously without the presence of a physician, offsetting diagnostic errors and further assisting clinicians in determining treatment plans for individuals affected with ET. Moreover, the implementation of a DNN-based approach in ET diagnostics presented by this thesis will augment teleoperative approaches by allowing individuals, who are unable to readily access a clinician for ET severity diagnosis, to remotely receive advanced levels of treatment for ET. And since the DNN-based approach presented by this thesis classifies ET in rapid succession, this approach will provide physicians an improved temporal understanding of ET.

Throughout the thesis, TETRAS was used as a metric standard for developing DNN training labels and datasets. Specifically, simulated and experimentally obtained signals were created and ranked based on the criteria outlined by TETRAS and [12]. Chapter 1 introduces the current state-of-art of ET severity diagnosis by introducing rating scales like FTM and TETRAS and exposing their faults. Particularly, TETRAS lacks robust assessment across the joint space and continual assessment of ET. Additionally, Chapter 2 utilizes the criteria outlined by TETRAS in Chapter 1 to generate and label experimental and simulated data for DNN training. Furthermore, Chapter 2 presents the experimental protocol used when creating experimental data.

In Chapter 3, the first iteration of eTETRAS was presented and tested using a single dimensional vector of knee angle measurements as training inputs into the DNN. This chapter demonstrates the DNN's effectiveness in classifying the severity of lower limb ET using signals obtained from an exoskeleton encoder. Chapter 4 builds on the findings of Chapter 3 by presenting a more robust version of eTETRAS. Unlike the first iteration, the second iteration uses a 2-dimensional vector of measurements as training inputs into the DNN. More specifically, stochastic calculus was employed to create a joint space model and concurrently used alongside knee angle measurements to train the DNN. Due to the introduction of an extra input and the fact that the input space of the machine learning model was now a robust Markov representation of the dynamic space, the second iteration of eTETRAS had significant improvements in classification accuracy than the first iteration of eTETRAS. Furthermore, the second iteration of eTETRAS demonstrated efficient classification ability, as evidenced by F1 scores and the confusion matrix.

5.1 Future Work

Although the proposed TETRAS-based classifiers demonstrate good training and validation accuracies, data obtained from a single test subject may limit the generalizability of the DNN, impeding its classification ability for a broader population. Hence, to enhance the DNN's generalizability and to cater to a wider demographic, a more diverse training dataset will be created in the future by including data from additional participants, particularly those diagnosed with lower limb ET. Additionally, employing different DNN training methodologies and architectures, such as implementing a dropout layer in the DNN, could help improve the generalizability of the DNN. These approaches aim to improve the model's effectiveness throughout a broader population. Due to the fact that Parkinsonian tremor and ET is difficult to distinguish [16, 17], future work could enable the classifier to distinguish between Parkinsonian tremor and ET, further assisting in physician diagnosis. Furthermore, this thesis, which focuses on lower limb ET during leg extension exercises, will extend its findings to classify additional parameters outlined in TETRAS, such as upper limb tremors, while also conducting further experiments involving participants with ET performing various exercises.

Bibliography

[1] CD Marsden. Movement disorders: Tremor. Book, 1984.

[2] Elan D Louis. Essential tremor. *The Lancet Neurology*, 4(2):100–110, 2005.

[3] WC Koller A Anouti. Tremor disorders. diagnosis and management. *The Western journal of medicine*, 1995.

[4] Thomas Welton, Francisco Cardoso, Jonathan A Carr, Ling-Ling Chan, Günther Deuschl, Joseph Jankovic, and Eng-King Tan. Essential tremor. *Nature Reviews Disease Primers*, 7(1):83, 2021.

[5] Mario Manto Giuliana Grimaldi. Neurological tremor: Sensors, signal processing and emerging applications. *Sensors (Basel, Switzerland)*, 2010.

[6] Franziska Hopfner, Dietrich Haubenberger, Wendy R Galpern, Katrina Gwinn, Ashlee Van't Veer, Samantha White, Kailash Bhatia, Charles H Adler, David Eidelberg, William Ondo, et al. Knowledge gaps and research recommendations for essential tremor. *Parkinsonism & related disorders*, 33:27–35, 2016.

[7] Annemarie Smid, Rik WJ Pauwels, Jan Willem J Elting, Cheryl SJ Everlo, J Marc C van Dijk, DL Marinus Oterdoom, Teus van Laar, Katalin Tamasi, AM Madelein van der Stouwe, and Gea Drost. A novel accelerometry method to perioperatively quantify essential tremor based on fahn–tolosa–marin criteria. *Journal of Clinical Medicine*, 12(13):4235, 2023.

[8] William Ondo, Vera Hashem, Peter A LeWitt, Rajesh Pahwa, Ludy Shih, Daniel Tarsy, Theresa Zesiewicz, and Rodger Elble. Comparison of the fahn-tolosa-marin clinical rating scale and the essential tremor rating assessment scale. *Movement Disorders Clinical Practice*, 5(1):60–65, 2018.

[9] Stanley Fahn, Eduardo Tolosa, Concepcíon Marín, et al. Clinical rating scale for tremor. *Parkinson's disease and movement disorders*, 2:271–280, 1993.

[10] Rodger Elble, Peter Bain, Maria João Forjaz, Dietrich Haubenberger, Claudia Testa, Christopher G Goetz, Albert FG Leentjens, Pablo Martinez-Martin, Anne Pavy-Le Traon, Bart Post, et al. Task force report: scales for screening and evaluating tremor: critique and recommendations. *Movement Disorders*, 28(13):1793–1800, 2013.

[11] Rodger J Elble. The essential tremor rating assessment scale. *Journal of Neurology & Neuromedicine*, 1(4), 2016.

[12] Stefano Calzetti, MARIO Baratti, M Gresty, and LESLIE Findley. Frequency/amplitude characteristics of postural tremor of the hands in a population of patients with bilateral essential tremor: implications for the classification and mechanism of essential tremor. *Journal of Neurology, Neurosurgery & Psychiatry*, 50(5):561–567, 1987.

[13] Bhomraj Thanvi, Nelson Lo, and Tom Robinson. Essential tremorthe most common movement disorder in older people. *Age and ageing*, 35(4):344–349, 2006.

[14] Rodger J Elble. Essential tremor frequency decreases with time. *Neurology*, 55(10):1547–1551, 2000.

[15] Rodger J Elble and William Ondo. Tremor rating scales and laboratory tools for assessing tremor. *Journal of the Neurological Sciences*, 435:120202, 2022.

[16] Samay Jain, Steven E Lo, and Elan D Louis. Common misdiagnosis of a common neurological disorder: how are we misdiagnosing essential tremor? *Archives of neurology*, 63(8):1100–1104, 2006.

[17] A Schrag, A Münchau, KP Bhatia, NP Quinn, and CD Marsden. Essential tremor: an overdiagnosed condition? *Journal of neurology*, 247:955–959, 2000.

[18] Allison Powell, Diane S Berry, Meagen Salinas, and Elan D Louis. Limb positioning and magnitude of postural tremor ratings: A study of 100 essential tremor cases. *Journal of the Neurological Sciences*, 445:120550, 2023.

[19] Fariborz Rahimi, Derek Debicki, Angela Roberts-South, Carina Bee, Priya Bapat, and Mandar Jog. Dynamic decomposition of motion in essential and parkinsonian tremor. *Canadian Journal of Neurological Sciences*, 42(2):116–124, 2015.

[20] J. T. Blackburn, D. R. Bell, M. F. Norcross, J. D. Hudson, and L. A Engstrom. Comparison of hamstring neuromechanical properties between healthy males and females and the influence of musculotendinous stiffness. *J. Electromyogr. Kinesiol.*, 19(5):e362–e369, October 2009.

[21] Olivia Samotus, Jack Lee, and Mandar Jog. Long-term tremor therapy for parkinson and essential tremor with sensor-guided botulinum toxin type a injections. *PLoS One*, 12(6):e0178670, 2017.

[22] Olivia Samotus, Fariborz Rahimi, Jack Lee, and Mandar Jog. Functional ability improved in essential tremor by incobotulinumtoxina injections using kinematically determined biomechanical patterns–a new future. *PloS one*, 11(4):e0153739, 2016.

[23] Basilio Vescio, Andrea Quattrone, Rita Nisticrianna Crasnd Aldo Quattrone. Wearable devices for assessment of tremor. *Frontiers in Neurology*, 12, 2021.

[24] Kathleen E Norman, Roderick Edwards, and Anne Beuter. The measurement of tremor using a velocity transducer: comparison to simultaneous recordings using transducers of displacement, acceleration and muscle activity. *Journal of neuroscience methods*, 92(1-2):41–54, 1999.

[25] Eus JW Van Someren, Myrthe D Pticek, Johannes D Speelman, Peter R Schuurman, Rianne Esselink, and Dick F Swaab. New actigraph for long-term tremor recording. *Movement disorders: official journal of the Movement Disorder Society*, 21(8):1136–1143, 2006.

[26] Dustin A. Heldman, Joseph Jankovic, David E. Vaillancourt, Janey Prodoehl, Rodger J. Elble, and Joseph P. Giuffrida. Essential tremor quantification during activities of daily living. *Parkinsonism Related Disorders*, 17(7):537–542, 2011.

[27] Donatas Lukšys, Gintaras Jonaitis, and Julius Griškevičius. Quantitative analysis of parkinsonian tremor in a clinical setting using inertial measurement units. *Parkinsons Disease*, 2018, 2018.

[28] Dayle Rüegge, Sujitha Mahendran, Lennart H Stieglitz, Markus F Oertel, Roger Gassert, Olivier Lambercy, Christian R Baumann, and Lukas L Imbach. Tremor analysis with wearable sensors correlates with outcome after thalamic deep brain stimulation. *Clinical Parkinsonism & Related Disorders*, 3:100066, 2020.

[29] Abdulnasir Hossen. A neural network approach for feature extraction and discrimination between parkinsonian tremor and essential tremor. *Technology and Health Care*, 21(4):345–356, 2013.

[30] Bryan T. Cole, Serge H. Roy, Carlo J. De Luca, and S. Hamid Nawab. Dynamic neural network detection of tremor and dyskinesia from wearable sensor data. In *2010 Annual International Conference of the IEEE Engineering in Medicine and Biology*, pages 6062–6065, 2010.

[31] Patrick Mcgurrin, James Mcnames, Tianxia Wu, Mark Hallett, and Dietrich Haubenberger. Quantifying tremor in essential tremor using inertial sensorsvalidation of an algorithm. *IEEE journal of translational engineering in health and medicine*, 9:1–10, 2020.

[32] Bryan T Cole, Serge H Roy, Carlo J De Luca, and S Hamid Nawab. Dynamical learning and tracking of tremor and dyskinesia from wearable sensors. *IEEE Transactions on Neural Systems and Rehabilitation Engineering*, 22(5):982–991, 2014.

[33] Giulana Grimaldi and Mario Manto. *Tremor: from pathogenesis to treatment.* Springer Nature, 2022.

[34] Sanghee Moon, Hyun-Je Song, Vibhash D Sharma, Kelly E Lyons, Rajesh Pahwa, Abiodun E Akinwuntan, and Hannes Devos. Classification of parkinsons disease and essential tremor based on balance and gait characteristics from wearable motion sensors via machine learning techniques: a data-driven approach. *Journal of neuroengineering and rehabilitation*, 17:1–8, 2020.

[35] Mehmet Engin, Serdar Demirag, Erkan Zeki Engin, Grbz lebi, Fisun Ersan, Erden Asena, and Zafer lakoglu. The classification of human tremor signals using artificial neural network. *Expert Systems with Applications*, 33(3):754–761, 2007.

[36] Xiaochen Zheng, Alba Vieira, Sergio Labrador Marcos, Yolanda Aladro, and Joaquín Ordieres-Meré. Activity-aware essential tremor evaluation using deep learning method based on acceleration data. *Parkinsonism & related disorders*, 58:17–22, 2019.

[37] Jihen Fourati, Mohamed Othmani, and Hela Ltifi. A hybrid model based on convolutional neural networks and long short-term memory for rest tremor classification. In *ICAART (3)*, pages 75–82, 2022.

[38] Luis Sigcha, Ignacio Pavon Costa, Susana Costa, Miguel Gago, Pedro Arezes, Juan Manuel L, and Guillermo De Arcas. Automatic resting tremor assessment in parkinsons disease using smartwatches and multitask convolutional neural networks. *Sensors*, 21(1), 2021.

[39] Yanwen Wang, Jiayu Yang, Miao Cai, Xiaoli Liu, Kang Lu, Yue Lou, and Zhu Li. Application of optimized convolutional neural networks for early aided diagnosis of essential tremor: Automatic handwriting recognition and feature analysis. *Medical Engineering Physics*, 113:103962, 2023.

[40] Clayton R. Pereira, Danillo R. Pereira, Joao P. Papa, Gustavo H. Rosa, and Xin-She Yang. *Convolutional Neural Networks Applied for Parkinson's Disease Identification*, pages 377–390. Springer International Publishing, Cham, 2016.

[41] Ayse Betul Oktay and Abdulkadir Kocer. Differential diagnosis of parkinson and essential tremor with convolutional lstm networks. *Biomedical Signal Processing and Control*, 56:101683, 2020.

[42] Christopher L Pulliam, SR Eichenseer, CG Goetz, Olga Waln, CB Hunter, J Jankovic, DE Vaillancourt, JP Giuffrida, and DA Heldman. Continuous in-home monitoring of essential tremor. *Parkinsonism & related disorders*, 20(1):37–40, 2014.

[43] Samit Bhanja and Abhishek Das. Impact of data normalization on deep neural network for time series forecasting. *arXiv preprint arXiv:1812.05519*, 2018.

[44] Ricky TQ Chen, Yulia Rubanova, Jesse Bettencourt, and David K Duvenaud. Neural ordinary differential equations. In *Advances in neural information processing systems*, pages 6571–6583, 2018.

[45] Jianbo B Gao. Analysis of amplitude and frequency variations of essential and parkinsonian tremors. *Medical and Biological Engineering and Computing*, 42:345–349, 2004.

[46] Christopher W. Hess and Seth L. Pullman. Tremor: Clinical phenomenology and assessment techniques. *Tremor and Other Hyperkinetic Movements*, 2012.

[47] T. Schauer, N. O. Negård, F. Previdi, K. J. Hunt, M. H. Fraser, E. Ferchland, and J. Raisch. Online identification and nonlinear control of the electrically stimulated quadriceps muscle. *Control Eng. Pract.*, 13(9):1207–1219, September 2005.

[48] Long Cheng, Yunpen Wang, Wei Ren, Zeng-Guang Hou, and Min Tan. On convergence rate of leader-following consensus of linear multi-agent systems with communication noises. *IEEE Trans. Autom. Control*, 61(11):3586–3592, 2016.

[49] M. Ferrarin and A. Pedotti. The relationship between electrical stimulus and joint torque: A dynamic model. *IEEE Trans. Rehabil. Eng.*, 8(3):342–352, September 2000.

[50] K. Bouyoucef and K. Khorasani. Robust feedback linearization-based congestion control using a fluid flow model. In *Proc. Am. Control Conf.*, pages 4882–4887, June 2006.

[51] Martin Burger, Peter Markowich, and Jan-Frederik Pietschmann. Continuous limit of a crowd motion and herding model: analysis and numerical simulations. *Kinet. Relat. Models*, 4(4):1025–1047, 2011.

[52] S. Bhasin. *Reinforcement Learning and Optimal Control Methods for Uncertain Nonlinear Systems*. PhD thesis, University of Florida, 2011.

[53] Fima C Klebaner. *Introduction to stochastic calculus with applications*. World Scientific Publishing Company, 2012.

[54] M Elizabeth H Hammond, Josef Stehlik, Stavros G Drakos, and Abdallah G Kfoury. Bias in medicine: lessons learned and mitigation strategies. *Basic to Translational Science*, 6(1):78–85, 2021.